Water soluble reactive phosphate (SRP) in atmospheric particles over East Mediterranean: The importance of dust and biomass burning events

Kalliopi Violaki, Irini Tsiodra, Athanasios Nenes, Maria Tsagkaraki, Giorgos Kouvarakis, Pavlos Zarmpas, Kalliopi Florou, Christos Panagiotopoulos, Ellery Ingall, Rodney Weber, et al.

Science of the Total Environment 830 (2022) 154263

Contents lists available at ScienceDirect

Science of the Total Environment

journal homepage: www.elsevier.com/locate/scitotenv

Water soluble reactive phosphate (SRP) in atmospheric particles over East Mediterranean: The importance of dust and biomass burning events

Kalliopi Violaki [a,b,*], Irini Tsiodra [b,c], Athanasios Nenes [a,c,e,*], Maria Tsagkaraki [b], Giorgos Kouvarakis [b], Pavlos Zarmpas [b], Kalliopi Florou [c], Christos Panagiotopoulos [d], Ellery Ingall [e], Rodney Weber [e], Nikos Mihalopoulos [b,f]

[a] Laboratory of Atmospheric Processes and their Impacts, School of Architecture, Civil & Environmental Engineering, École Polytechnique Fédérale de Lausanne, Lausanne 1015, Switzerland
[b] Environmental Chemical Processes Laboratory (ECPL), Chemistry Department, University of Crete, 71003 Heraklion, Crete, Greece
[c] Center of Studies on Air quality and Climate Change (C-STACC), Institute of Chemical Engineering Sciences, Foundation for Research and Technology, Hellas, Patras, Greece
[d] Aix Marseille Univ., Université de Toulon, CNRS, IRD, MIO, Marseille, France
[e] School of Earth and Atmospheric Sciences, Georgia Institute of Technology, Atlanta, GA, 30332, United States of America
[f] Institute for Environmental Research and Sustainable Development, National Observatory of Athens, Pendeli, Greece

HIGHLIGHTS

- Soluble reactive P was measured online with a time resolution of a few minutes.
- Saharan dust is an important primary source of bioavailable P.
- The acid dust enhances the dust aerosol contribution to the soluble reactive P.
- Biomass burning contributes significantly to soluble P in the area during summer.

GRAPHICAL ABSTRACT

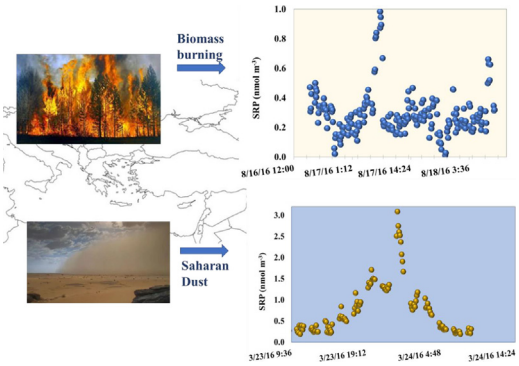

ARTICLE INFO

Article history:
Received 14 November 2021
Received in revised form 2 February 2022
Accepted 27 February 2022
Available online 02 March 2022

Editor: Pavlos Kassomenos

Keywords:
Soluble reactive phosphate
Dust
Biomass burning
PILS
Biogeochemical P cycle

ABSTRACT

The importance of dust and biomass burning episodes on the atmospheric concentration of water-soluble reactive phosphate (SRP) was determined in the eastern Mediterranean. SRP was measured with a new rapid real-time automated analytical system with a time resolution of a few minutes per sample and with an extremely low detection limit. The average atmospheric concentration of SRP during the sampling campaign was estimated at 0.35 ± 0.25 (median 0.30) nmol P m^{-3}. The maximum concentration of SRP (3.08 nmol P m^{-3}) was recorded during an intense dust episode, and was almost ten times higher than the campaign average, confirming that Saharan dust was an important primary source of bioavailable P to the eastern Mediterranean, especially during the spring period when 60% of the events occurred. Predicted increases in the frequency and intensity of dust storms in the area will enhance the role of the atmosphere as a source of bioavailable P for the Mediterranean marine ecosystem. During the warm period, when Northerly winds prevailed, biomass burning processes contributed significantly to soluble phosphorus delivered from atmospheric sources to the eastern Mediterranean. These inputs during warm periods are especially important for the Eastern Mediterranean, where biological productivity is strongly limited by nutrient availability.

* Corresponding authors at: Laboratory of Atmospheric Processes and their Impacts, School of Architecture, Civil & Environmental Engineering, École Polytechnique Fédérale de Lausanne, Lausanne 1015, Switzerland.
E-mail addresses: kalliopi.violaki@epfl.ch (K. Violaki), athanasios.nenes@epfl.ch (A. Nenes).

http://dx.doi.org/10.1016/j.scitotenv.2022.154263

1. Introduction

The link between phosphorus (P) availability, marine net primary productivity, oceanic carbon uptake and climate have motivated considerable interest into the study of orthophosphate abundance and dynamics, since it is the most bioavailable form of P (Karl and Björkman, 2015). Orthophosphate is readily soluble in water and can promote phytoplankton growth, especially in phosphorus-limited marine environments (Okin et al., 2011). The atmosphere is considered an important pathway for supplying primary phosphate ions to the surface aquatic systems (Guerzoni et al., 1999; Herut et al., 2002), with mineral dust the principal phosphate source globally, contributing 48% of the total P supply to the oceans (0.115 Tg P a^{-1}) (Mahowald et al., 2008). Additionally, recent study showed that apart from the dust, bioaerosols consist an important source for phosphate ions (Violaki et al., 2021).

Observations suggest that the labile fractions of nutrients, such as P, are higher during atmospheric transport, at least in part, due to exposure to acidic (i.e., low pH) conditions in aerosol or cloud waters (Baker et al., 2021). The acid-driven P solubilization due to dust acidification could significantly enhance the bioavailable P deposition (Nenes et al., 2011; Stockdale et al., 2016). The phosphorus cycle is also modulated by combustion-related emissions, providing more soluble P and impacting primary production in marine ecosystems (Wang et al., 2015; Barkley et al., 2019).

The East Mediterranean Sea (EMS) is a crossroads of air masses with vastly different influences. It receives significant amounts of mineral aerosol from the Sahara desert and polluted air masses from northern Europe which are rich in both oxidants, inorganic and organic acids. The mixture of these air masses in different proportions is expected to show a range of different phosphate ions sources. Furthermore, the EMS is P limited in the winter and N, P co-limited for phytoplankton in summer (Krom et al., 2016; Pitta et al., 2017). The results of microcosm bioassay manipulations with EMS surface water on which acidified Saharan dust was added suggested that the acid processes in the atmosphere will increase the amount of labile P (Krom et al., 2016).

Most atmospheric phosphate ions data reported for the EMS (Markaki et al., 2003; Nenes et al., 2011) is based on filter sampling, with time resolution of typically 1 to 3 days. However, such long sampling durations could introduce artifacts, like mixing of aerosol from different sources on the filter, and possible reactions on the filter that would promote additional dissolution of P. Furthermore, the low temporal resolution does not allow the detection of phosphate solubility changes during the evolution of a plume, which hampers a full understanding of how acidification impacts the flux of soluble P in each plume transition event.

To address these issues, we developed a rapid real-time automated analytical system to measure the soluble reactive phosphate (SRP) in atmospheric particles with a time resolution of a six minutes per sample and with detection limit of 0.4 nM P (Violaki et al., 2016). Here we present results of the first long-term deployment of the SRP measurement system, during an eight-month operational period in 2016 at a location in the center of the EMS (Crete, Greece). During the sampling period, a number of Sahara dust outbreaks and biomass burning episodes (BB) were sampled. The events were compared in terms of the contribution to overall atmospheric pool of SRP, while the role of acidification as a modulator of SRP dissolution was investigated. The biogeochemical implications of the events are discussed and the contribution of dry deposited phosphate to the new production in the EMS is estimated.

2. Material and methods

2.1. Sampling area

The sampling was operated during a period of eight months (January–April and June–September 2016) on the roof of University of Crete at Heraklion, Greece and three days (May 11–13, 2016) at the Finokalia sampling station. The Finokalia station (35o 20′ N, 25o 40′ E, 250 m asl) is away from direct urban influence (Fig. 1) and is representative of background measurements in the eastern Mediterranean, with air masses most commonly originating from continental Europe and northern Africa (Sahara

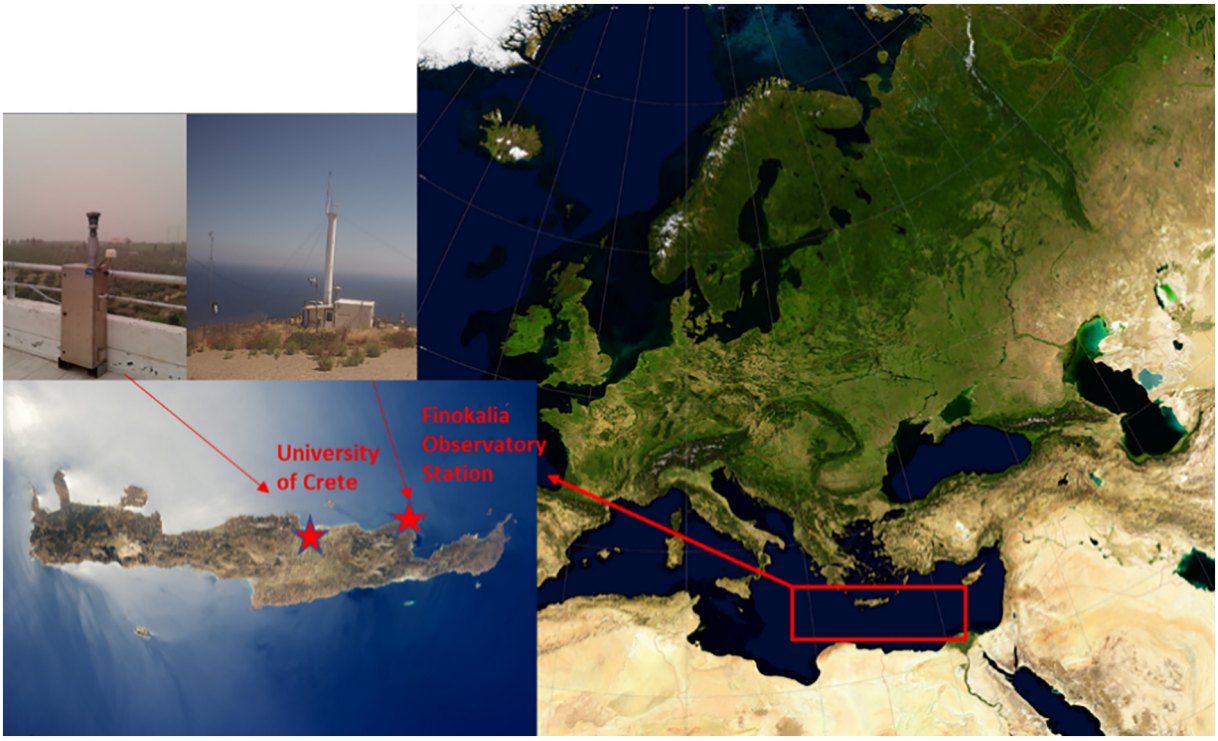

Fig. 1. Heraklion (35°30′ N, 25°13′ E) and Finokalia sampling stations (35°20′ N, 25°40′ E).

desert), especially during spring and autumn. More details on Finokalia and the prevailing site climatology can be found at http://finokalia.chemistry.uoc.gr/ and Mihalopoulos et al. (1997). The sampling site in Heraklion (Fig. 1) was at the northern part of the Department of Chemistry, University of Crete, (35°18′ N, 25°45′ E) located in a rural area approximately 6 km from Heraklion and 54 km from the Finokalia station.

2.2. PILS-LWCC system and $PM_{2.5}$ aerosol sampling

The PILS-LWCC system consists of one Particle-Into-Liquid Sampler (PILS), two peristaltic pumps (8-channel and 4-channel from ISMATEC), a 250 cm long path length Liquid Waveguide Capillary Cell (LWCC), and two two-position fluid valve processors (Alltech, Inc.). The concentration of phosphate in the sample is determined by measuring the absorbance of the phosphomolybdenum blue complex in the LWCC at 690 nm using light from a dual deuterium and tungsten halogen light source (DT-Mini-2, Ocean Optics). More details for the on-line measurement of SRP, the chemical reaction and the reagents are available in Violaki et al. (2016). The detection limit (DL) of the system estimated by three times the standard deviation of the measurement blanks ($n = 15$), was 0.4 nM P, which is equivalent to 0.03 nmol P m^{-3} in atmospheric particles under the given sampling conditions. The standard uncertainty of the blank was 4%. This method measures the dissolved (i.e., which passes through a 0.45 μm pore size filter) phosphate and it is called hereafter "soluble reactive phosphate" (SRP).

$PM_{2.5}$ aerosol filter samples were collected in Heraklion ($n = 362$) and in the Finokalia sampling station ($n = 37$). The samples were collected on Teflon filters (PALL, Zerfluor, 2 μm pore size, 47 mm diameter) using an automated sampler (PNS 16T-3.1, Gomde-Derenda) with air flow rate of 2.3 $m^3\ h^{-1}$. The sampling was performed once a week following the sampling of the on line PILS-LWCC system and focused on sampling the dust events during spring season and biomass burning episodes during summer. The resolution time of sampling was 3 h. Upon collection, the filters were stored at −18 °C until analysis, which was performed no longer than one month after collection.

2.3. Analysis of main ions and Total Phosphorus (TP)

Half of the teflon filter (PALL, 47 mm) was extracted with 10 mL of ultrapure water (Milli-Q system, 18 MΩ.cm) by sonication for 45 min. The extracted samples were filtered with a 0.45 μm Sartorious polypropylene syringe filter (25 mm diameter) and then analyzed with ion chromatography (IC). The main anions (chloride, nitrate sulfate, phosphate, and oxalate) in aerosol extracts were separated with a Dionex AS4A-SC column. All the anions were determined with isocratic elution at 1.5 mL min^{-1} of Na_2CO_3/$NaHCO_3$ eluent and an ASRS-300 4 mm suppressor in autosuppression mode. For the cations (sodium, ammonium, potassium, magnesium, calcium) a CS12-SC column was used with a CSRS-300 4 mm suppressor. Separation was achieved under isocratic conditions with MSA (20 mM) eluent and flow rate of 1.0 mL min^{-1}. The reproducibility of the measurements was better than 2% and the detection limit ranged from 1 to 5 ppb for the main anions and cations. The detection limit of HPO_4^{2-} was 3 ppb and blanks were always below the detection limits. Dissolved (<0.45 μm) phosphate ions measured with the IC will hereafter be referred to as the operational term "phosphate".

TP in $PM_{2.5}$ aerosol samples collected during the dust event on 23th March 2016 was determined according to the analytical protocol in Violaki et al. (2018). TP was measured with persulfate digestion method, converting all P forms to PO_4^{3-} and measured colorimetrically as PO_4^{3-} at 690 nm using the stannous chloride method. TP recoveries obtained by the use of certified reference materials (MESS-3) were found to be 98 ± 12%.

2.4. AMS instrument

The chemical composition of the non-refractory submicron particulate mass was measured in real-time by an Aerodyne high resolution time-of-flight-aerosol mass spectrometer (HR-ToF-AMS) only in Finokalia sampling station. The concentrations of the major PM_1 components were measured every 3 min using both mass spectrum (MS) and particle time of flight data (pToF). In this study only V-mode data were obtained. The heater was operating at 600 °C for the aerosol thermal desorption and the tungsten filament for electron ionization was at 70 eV. All HR-ToF-AMS data were analyzed using the standard AMS software toolkit (SeQUential Igor data RetRiEvaL; SQUIRREL v1.56D), while the high-resolution data were processed using the Peak Integration by Key Analysis (PIKA v1.15D, available at: http://cires1.colorado.edu/jimenez-group/wiki/index.php/High_Resolution_ToFAMS_Analysis_Guide) software, within Igor Pro 6 (Wave Metrics). A time-dependent collection efficiency has been applied to our HR AMS data during the campaign. This collection efficiency was calculated according to the algorithm of Kostenidou et al. (2007), which combines the AMS PTOF mass distributions and the SMPS volume distributions and was on average 0.64.

2.5. Calculation of aerosol acidity

The ISORROPIA-II thermodynamic model (https://isorropia.epfl.ch/; Nenes et al., 1998; Fountoukis and Nenes, 2007) was used to constrain the levels of bulk aerosol acidity. This model calculates the composition of aerosol in equilibrium with the surrounding gas phase, including the transformations taking place when freshly emitted dust is mixed with acidic pollution. The model takes as input the amount of "aerosol precursor" sodium, potassium, ammonium, sulfate, magnesium, calcium, chloride, nitrate, relative humidity and temperature. The concentrations (in μg m^{-3}) of these precursors refer to the total amount in the gas and aerosol phases. Based on this input the model predicts, at thermodynamic equilibrium, the phases present in the aerosol particles (aqueous, solid, or both), the amount and chemical composition of each phase, and, the concentrations of semivolatile species in the gas phase (NH_3, HNO_3, HCl). Here, ISORROPIA-II was run in the "forward mode" assuming a metastable aerosol state, in which known quantities are temperature, relative humidity and the total (i.e., gas + aerosol) concentrations of NH_3, H_2SO_4, HCl and HNO_3. The equilibrium assumption applies well to submicron (fine) aerosol but introduces errors when applied to coarse mode aerosol (Capaldo et al., 2000; Pye et al., 2020). Nevertheless, it can still provide a good indicator of changes in acidity – as is done here. The particle pH calculated here is based on the calculated equilibrium particle hydronium ion concentration in the aerosol and does not account for the organic aerosol liquid water content.

3. Results

3.1. High resolution measurements of SRP in Heraklion

The temporal variability of SRP concentration measured with the PILS-LWCC at campus of University of Crete (Heraklion, Greece) during January–April and June–September 2016 is presented in Figs. 2a & 3a, respectively. The system measured almost each week for two or three days continuously, performing in total 5062 measurements with 6 min time resolution. The total average concentration of SRP during the sampling campaign was estimated at 0.35 ± 0.25 (median: 0.30, $n = 5062$) nmol P m^{-3}, with standard uncertainty of 0.3%. These levels of SRP agree with previous filter-based phosphate measurements (median 0.23 nmol m^{-3}) in the same area (Markaki et al., 2003) but also in Erdemli (0.45 ± 0.43 nmol m^{-3} median 0.37 nmol m^{-3}) for bulk aerosols (Koçak et al., 2010).

The sampling period could be separated in two seasons; the season of high dust influence (Jan.-April) and the season with high biomass burning events (June–September). The temporal variation of SRP together with PM_{10} mass during the season of high dust influence is shown in Fig. 2a. During the intense dust episode recorded on 23th of March (Fig. 2b & c) we observed the maximum recorded concentration of non-sea salt (nss)-calcium (16.94 μg m^{-3}, Fig. S1), which was 14 times higher than the background levels (1.22 ± 1.56 μg m^{-3}, Koulouri et al., 2008), and also the maximum

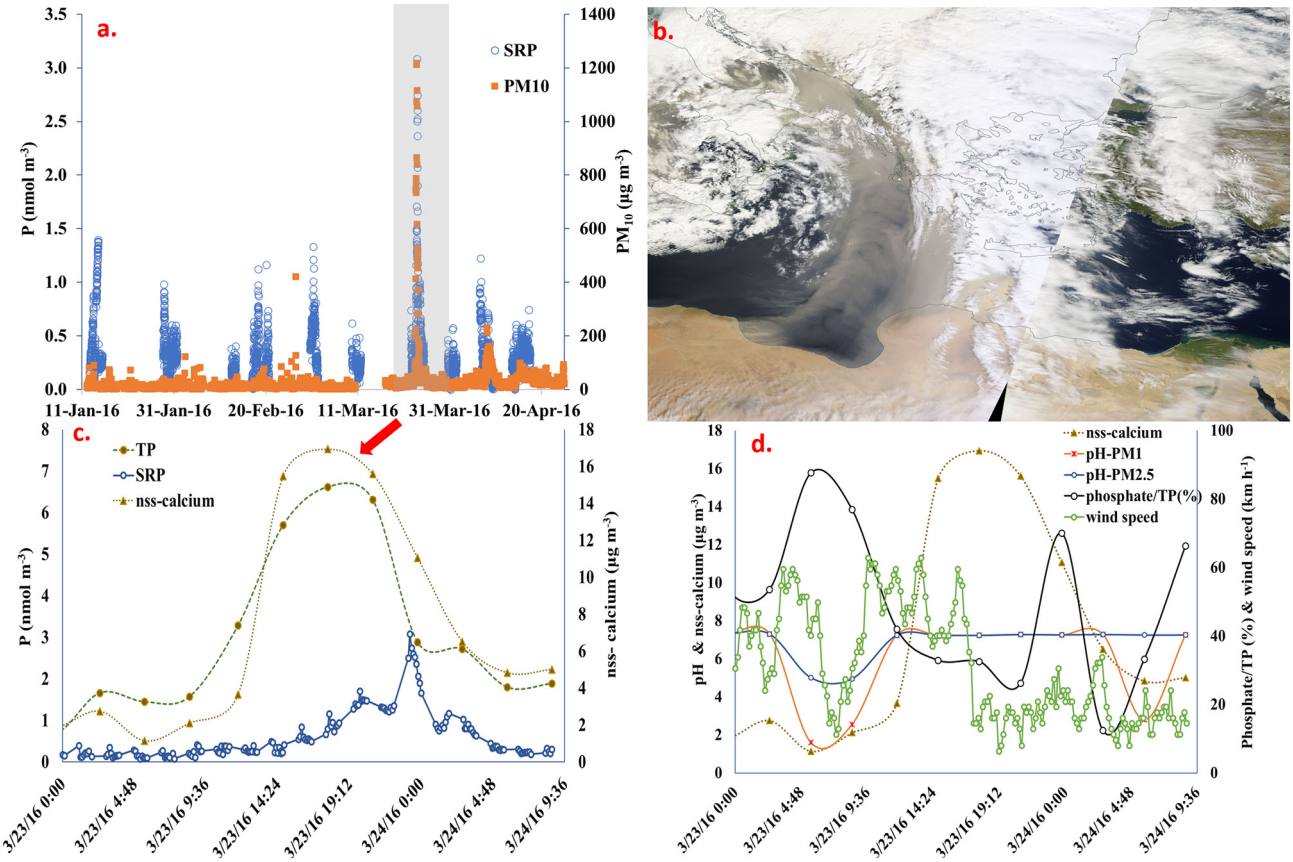

Fig. 2. a) The temporal variation of SRP concentrations measured with the PILS-LWCC system from January to April 2016, in parallel with the PM_{10} mass at campus of University of Crete (Heraklion, Greece), b) the satellite picture depicts the transportation of Saharan dust peaked on 23th of March 2016; the picture was downloaded from "NASA Worldview" (https://worldview.earthdata.nasa.gov/), c) Total P (TP) during the dust event on 23th of March 2016 along with SRP and nss-calcium, d) the solubility of phosphate (ratio phosphate: TP) during the dust event with pH in $PM_{2.5}$ particles (pH-PM2.5) and the pH in PM_1 particles (pH-PM1), nss-calcium and wind speed (km h^{-1}). pH was calculated by the ISORROPIA-II thermodynamic model (Fountoukis and Nenes, 2007) using the observed ionic composition, while the pH in PM_1 particles was calculated based on size segregated results obtained during similar dust event in the area (Table S6).

PM_{10} mass (1218 μg m^{-3}) which was 24 times higher than the annual average PM_{10} levels for Heraklion (51 ± 33 μg m^{-3}, Gerasopoulos et al., 2006). The duration of that dust event was about 24 h and the variation of SRP could be resolved during this event since an online measurement was recorded every 6 min (Fig. 2c). The maximum concentration of SRP (3.08 nmol P m^{-3}) was recorded during this dust event, being almost ten times higher than the campaign average (0.35 ± 0.25 nmol P m^{-3}). Total Phosphorous (TP) was measured on Teflon filters that were collected only during that dust event (Fig. 2c). The average TP was 2.75 ± 1.97 nmol P m^{-3}, being a maximum (6.62 nmol P m^{-3}) at the peak of nss-calcium. This average is a typical value for an intense dust event in the area (Longo et al., 2014; Violaki et al., 2021).

Nine biomass burning events were recorded during the June–September period. During biomass burning events high concentrations of nss-potassium were observed, often concurrently with dust (when the concentration of nss-calcium was higher than 1 μg m^{-3}). The co-occurrence of nss-potassium and nss-calcium makes it difficult to differentiate the contribution of biomass from dust to phosphate concentration. Two biomass burning events, however, were recorded without dust influence and with low concentration of nss-calcium; the first was on 17th Aug. 2016 with nss-calcium: 0.07 ± 0.02 μg m^{-3} (Fig. 3c) and the second was on 26th Aug. 2016 with nss-calcium:0.08 ± 0.02 μg m^{-3} (Fig. 3d). The maximum recorded SRP concentration during those events was 1.46 and 0.98 nmol P m^{-3}, respectively, being 3 to 4 times higher than the campaign average (0.35 ± 0.25 nmol P m^{-3}), suggesting that biomass burning could be an important source of phosphate over East Mediterranean, especially during periods where dust is absent (i.e., Northern winds called Etesians are prevalent, Fig. S2).

3.2. High resolution measurements of SRP and ancillary parameters in Finokalia sampling station

During the sampling period at Finokalia (from 11th to 13th May 2016), an AMS system measuring PM_1 SO_4^{2-}, along with NH_4^+, NO_3^- and Cl^- (with a temporal resolution of 3 min) was deployed in parallel with the PILS system. The temporal variability of both parameters is presented in Fig. 4, along with PM_{10} mass and pH, calculated by the ISORROPIA-II model (Fountoukis and Nenes, 2007). Over these two days sampling at high resolution, we had the opportunity to compare the two primary sources of SRP over EMS; anthropogenic activities and the Saharan dust. The daily average of sulfate concentration recorded during 11th May was higher (4.44 ± 0.93 μg m^{-3}) comparing with the daily average on the 12th May (0.48 ± 0.28 μg m^{-3}). This is probably attributed to anthropogenic activities, since during that day the wind origin was from the North and Northeast Europe (Fig. 4), while the calculated acidic pH (1.6 ± 1.3) was driven by the aerosol sulfate. The temporal variation of SRP on 11th May (peaking at 0.85 nmol P m^{-3}) is in line with the sulfate trend. The peak on 12th May (1.00 nmol P m^{-3}) follows the temporal trends of PM_{10} (Fig. 4) and nss-calcium (Fig. S3) suggesting that dust could be the source of the second observed maximum of SRP. The dust event is also confirmed by the air mass back trajectories (Fig. 4), while the average pH was calculated at 7.2 (owing to a surplus of calcium, presumably in the form of carbonates). Although the sampling period was short, these measurements suggest that anthropogenic activities could be a comparable source of SRP to a low intensity dust event.

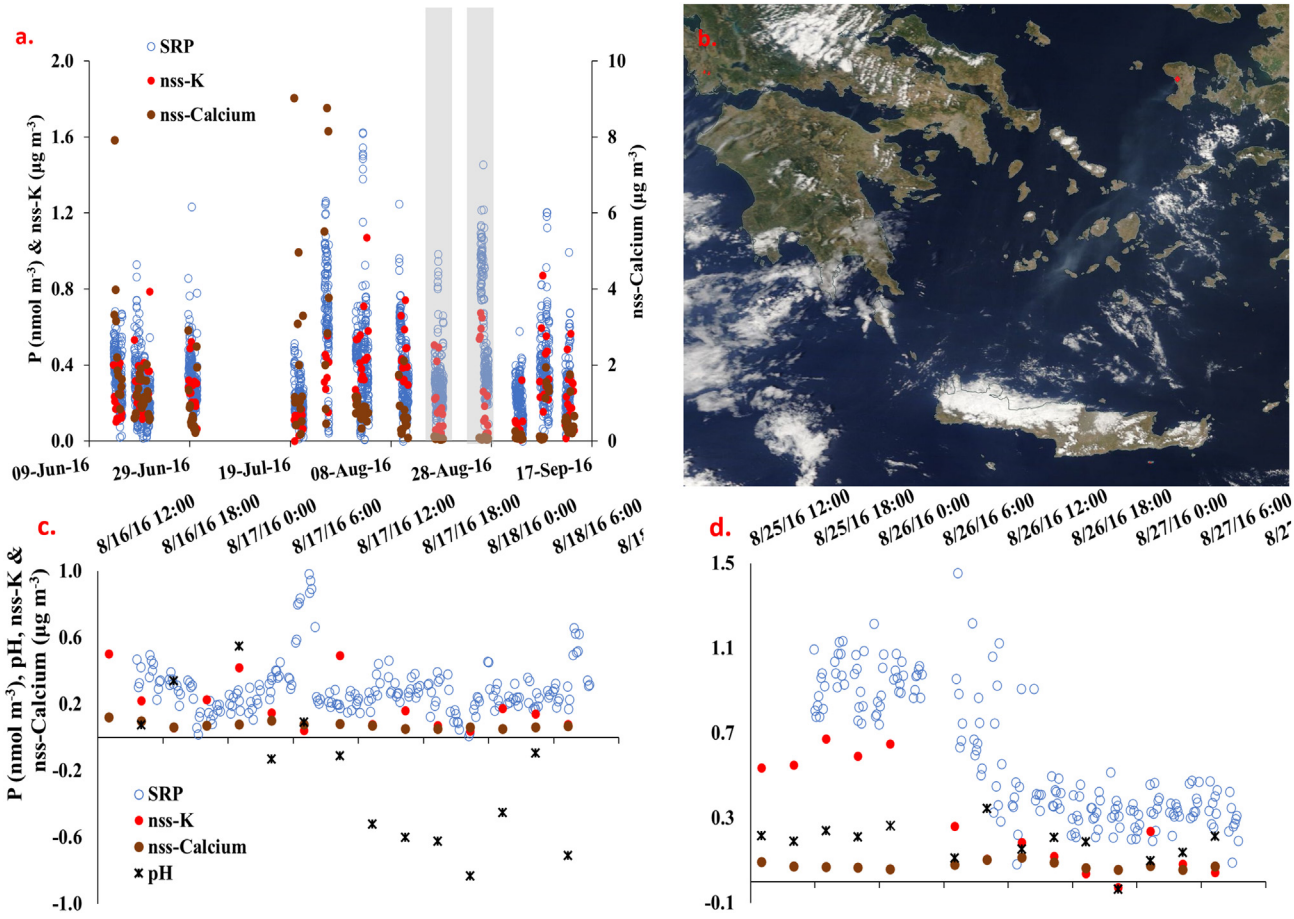

Fig. 3. a) Temporal variation of SRP concentration measured with the PILS-LWCC system during June to September 2016; nss-calcium and nss-potassium were measured in $PM_{2.5}$ aerosol filters sampled in parallel at campus of University of Crete (Heraklion, Greece), b) the biomass burning episode on 26–27th August 2016 in Chios island, which recorded from satellite; the picture was downloaded from "NASA Worldview" (https://worldview.earthdata.nasa.gov/) on 26th August 2016, c) focus on the temporal variation of SRP concentration, nss-calcium and nss-potassium and pH during the biomass burning episode on 17–18th August 2016 in Kefalonia island, d) focus on the temporal variation of SRP concentration, nss-calcium and nss-potassium and pH during the biomass burning episode on 26–27th August 2016 in Chios island. The pH was calculated by the ISORROPIA-II thermodynamic model (Fountoukis and Nenes, 2007), using the ionic composition.

4. Discussion

4.1. The seasonal influence of air mass origin to the phosphate ions and atmospheric pH

The average concentration of various parameters, including pH and SRP for different seasons and main air mass origin for species transported to the sampling site is summarized in Table 1. The average pH in $PM_{2.5}$ atmospheric particles during dust events in winter, spring and summer was calculated at 7.26 ± 0.05 (median: 7.3), consistent with a surplus of calcium in the form of carbonates. In autumn, no dust events were recorded during the sampling period. Significant correlation was found in dust events between phosphate and nss-calcium ($r = 0.64$, $p < 0.0001$, Table S1), nss-magnesium ($r = 0.65$, $p < 0.0001$, Table S1) and chloride ($r = 0.64$, $p < 0.0001$, Table S1), suggesting the transport of phosphate with Saharan dust (Mahowald et al., 2008) in boundary layer over the Mediterranean Sea.

The atmospheric particles are considerably more acidic with pH at 3.72 ± 2.76, when the anthropogenic influence is dominant with winds blowing from central Europe during summer. Particles are even more acidic when originating from countries bordering the Black Sea, with pH at 1.70 ± 2.15 during the same season. Those air masses were associated with the highest average concentration of phosphate over the East Mediterranean, especially during the spring (0.84 ± 0.42 nmol P m^{-3}) and summer periods (0.52 ± 0.36 nmol P m^{-3}). The Black Sea wind sector is characterized not only by strong anthropogenic emissions (Koçak et al., 2016), but also from biomass burning emissions (Sciare et al., 2008); the highest concentration of nss-sulfate ions (4.35 ± 2.00 μg m^{-3}) and nss-potassium (0.35 ± 0.21 μg m^{-3}) originated from that sector (Table 1).

4.2. The role of acid processing of dust on the levels of phosphate ions

Dust events are an important primary source of bioavailable phosphorus, but when the dust is acid processed, it could produce considerable amounts of secondary phosphate anions from the dissolution of apatite, which can increase inorganic P by 10 times (Nenes et al., 2011; Stockdale et al., 2016). To investigate the effect of dust acidification on phosphate levels, we estimated the "phosphate solubility" (molar ratio PO_4^{3-}: TP) during the intense dust event recorded on 23th of March 2016 (Fig. 2b). Indeed, we see that pH drops at the edge of the plume (Fig. 2d) and corresponds to a much higher solubility (82%) compared to the peak of the event with average solubility 30% and pH = 7 (Fig. 2d). This pattern is consistent with the expectation that smaller amounts of dust occurring at the edge of the event are efficiently mixed with anthropogenic pollution, leading to much higher acid exposure (and reduced pH) compared to the peak of the plume. The higher acid exposure at the flanks of the dust plume leads to higher phosphate solubility, compared to within the center or peak of the plume. This process seems to be facilitated by the low wind speed, which was recorded at the beginning of the event, supporting long processing times with acids, increasing the acid solubilization of dust (Fig. 2d). It is expected that pH varies with particle size (Kakavas et al., 2021) especially during dust episodes. For this reason, during periods where ISORROPIA yields high pH (indicative of a surplus of non-volatile cations (NVCs) e.g., Na, Ca, Mg, K, which cannot be fully "neutralized"

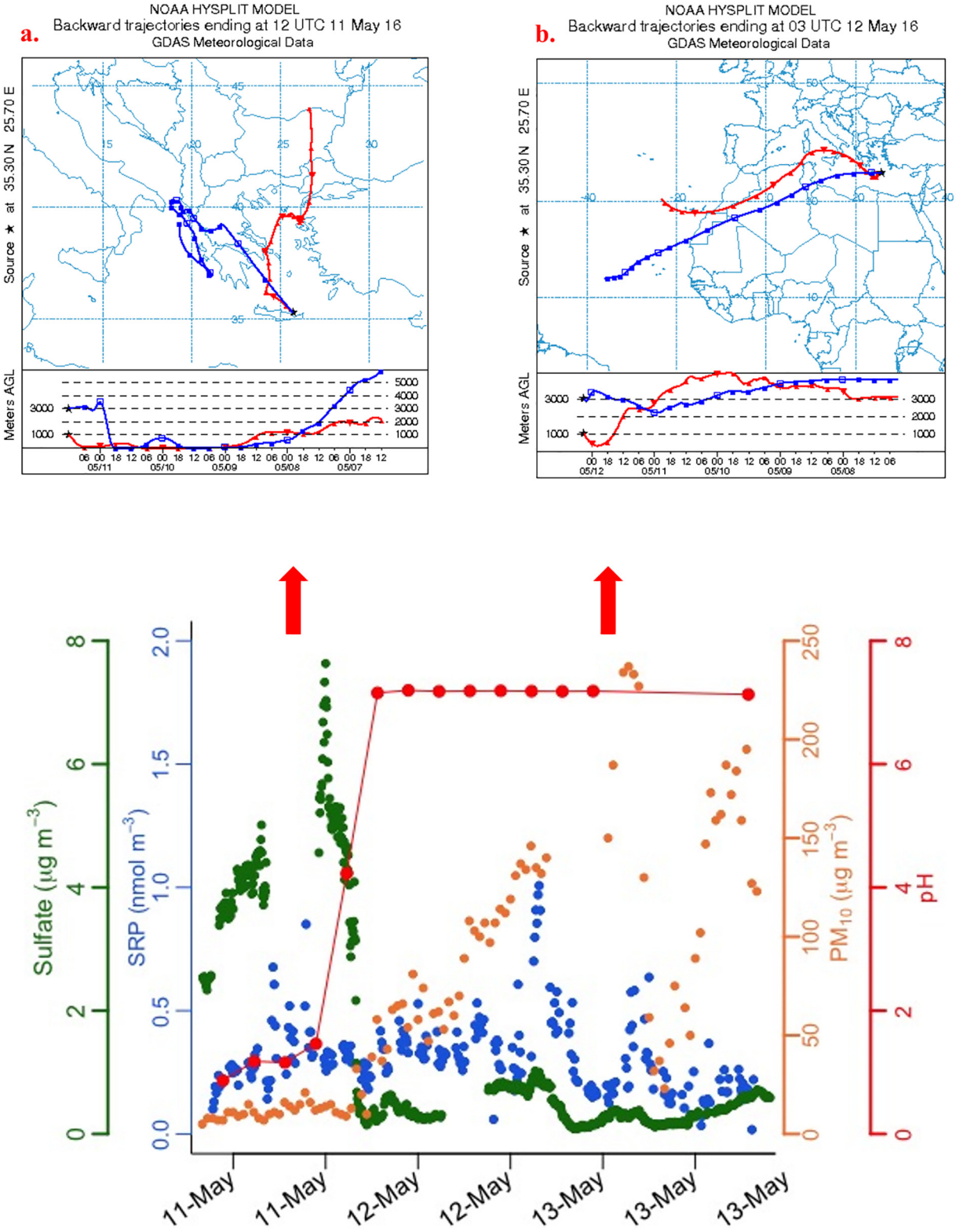

Fig. 4. Concentration of SRP measured with the PILS-LWCC system in $PM_{2.5}$ atmospheric particles, sulfate measured with AMS in PM_1 atmospheric particles and PM_{10} mass during the sampling in Finokalia (11th–13th May 2016). The pH was calculated by the ISORROPIA-II thermodynamic model (Fountoukis and Nenes, 2007). The air mass back trajectories on a) 11th May 2016 and b) 12th May 2016 were calculated for 1000 m and 3000 m with 6 h step by using the HYSPLIT Model (Stein et al., 2015).

by anions), it would be useful to assess whether smaller particles are more acidic and their associated P subject to solubilization. For this, we estimate the fraction of NVCs in PM_1, considering the size segregated measurements of NVCs during dust events occurred in the area (Table S6). The estimated fraction of the species in PM_1 was applied to the $PM_{2.5}$ data and was used to estimate the pH in PM_1 particles using ISORROPIA-II (Fig. 2d). The lower pH in PM_1 particles (pH = 1.61) at the begging of event implies that the solubilization of dust was likely complete in the fine particles, while the modest variability in pH in PM_1 particles during the dust episode indicate an underlying acidification that may be underway. Nevertheless, a lack of more size-

Table 1
Average concentration of various parameters including pH and phosphate ions distributed to the main air masses origin in the area. All concentrations are in μg m^{-3}, except phosphate ions in nmol m^{-3}. All parameters were measured in $PM_{2.5}$ teflon filters. The pH was calculated by the ISORROPIA-II thermodynamic model (Fountoukis and Nenes, 2007), using the ionic composition. The molar ratio PO_4^{3-}: nss-Ca^{2+} also presented. Note that winter define here from January to February, spring is defined by the period from March to May, summer is the period from June to August and in autumn is included only September.

		pH-$PM_{2.5}$	nss-Ca^{2+}	NH_4^+	NO_3^-	nss-SO_4^{2-}	nss-K^+	PO_4^{3-}	PO_4^{3-}: nss-Ca^{2+}
Winter	Dust (n = 23)	7.26 ± 0.05	0.61 ± 0.42	0.18 ± 0.13	0.54 ± 0.39	0.34 ± 0.31	0.17 ± 0.12	0.32 ± 0.30	0.02
	Acid dust (n = 3)	3.88 ± 0.27	0.24 ± 0.05	0.08 ± 0.03	0.70 ± 0.16	0.28 ± 0.03	0.09 ± 0.08	0.18 ± 0.11	0.03
	Cent. Europe (n = 28)	3.81 ± 2.93	0.26 ± 0.12	0.36 ± 0.28	0.76 ± 0.57	1.53 ± 1.38	0.31 ± 0.18	0.33 ± 0.29	0.05
	Black Sea (n = 2)	0.85 ± 1.39	0.16 ± 0.00	0.86 ± 0.79	1.32 ± 0.36	3.47 ± 0.23	0.22 ± 0.17	0.19 ± 0.00	0.05
	Marine (n = 1)	7.26	0.39	0.08	0.33	0.12	0.08	0.41	0.04
Spring	Dust (n = 44)	7.27 ± 0.06	4.13 ± 3.89	0.54 ± 0.49	1.95 ± 1.73	2.47 ± 1.43	0.28 ± 0.18	0.88 ± 0.54	0.01
	Acid dust (n = 32)	3.27 ± 1.27	0.76 ± 0.45	0.83 ± 0.35	1.40 ± 0.76	2.86 ± 1.22	0.28 ± 0.14	0.55 ± 0.37	0.03
	Cent. Europe (n = 6)	3.70 ± 1.27	0.52 ± 0.53	0.82 ± 0.86	1.34 ± 0.91	2.50 ± 1.90	0.39 ± 0.09	0.47 ± 0.28	0.04
	Black Sea (n = 5)	1.72 ± 0.26	0.57 ± 0.21	1.14 ± 0.33	1.48 ± 1.23	3.28 ± 1.19	0.31 ± 0.14	0.84 ± 0.42	0.06
	Marine (n = 12)	3.74 ± 2.27	0.46 ± 0.30	0.73 0.41	0.87 0.64	1.68 ± 1.03	0.27 ± 0.16	0.53 ± 0.34	0.05
Summer	Dust (n = 7)	7.18 ± 0.06	2.67 ± 2.44	0.68 ± 0.11	0.91 ± 1.14	1.67 ± 1.70	0.34 ± 0.43	0.36 ± 0.25	0.01
	Acid dust (n = 6)	2.73 ± 1.33	0.92 ± 0.28	1.01 ± 0.17	0.48 ± 0.27	3.60 ± 1.01	0.28 ± 0.14	0.38 ± 0.33	0.02
	Cent. Europe (n = 36)	3.72 ± 2.76	1.24 ± 1.07	0.57 ± 0.48	0.77 ± 0.51	2.93 ± 1.68	0.22 ± 0.15	0.69 ± 0.40	0.02
	Black Sea (n = 73)	1.70 ± 2.15	0.82 ± 1.46	0.92 ± 0.70	0.55 ± 0.32	4.35 ± 2.00	0.35 ± 0.21	0.52 ± 0.36	0.03
	Marine (n = 1)	6.11	1.74	0.79	1.53	3.59	0.12	0.25	0.01
Autumn	Dust (n = 0)	–	–	–	–	–	–	–	
	Acid dust (n = 4)	1.82 ± 0.48	1.21 ± 0.39	1.34 ± 0.59	0.61 ± 0.43	5.00 ± 1.98	0.26 ± 0.19	0.38 ± 0.25	0.01
	Cent. Europe (n = 22)	1.07 ± 1.23	0.44 ± 0.63	0.79 ± 0.70	0.59 ± 0.40	4.41 ± 2.60	0.25 ± 0.22	0.55 ± 0.44	0.05
	Black Sea (n = 8)	0.65 ± 1.00	0.32 ± 0.17	1.04 ± 0.55	0.68 ± 0.65	4.55 ± 1.24	0.24 ± 0.16	0.30 ± 0.17	0.04
	Marine (n = 1)	−0.14	0.53	0.83	0.46	3.45	0.08	1.94	0.15

resolved data cannot conclusively show this, so we refer to future work for constraining much better the size-resolved pH and further the solubility of phosphate.

A 5-year climatology study (Kalivitis et al., 2007) in the area showed that Saharan dust arrives over Crete in three possible ways: a) vertically extended transport, where dust between 1000 m and 3000 m is transported b) free tropospheric transport where, dust is transported at altitudes of 3000 m and above, and, c) boundary layer transport where, dust is transported at altitudes up to 1000 m. The dust events occurring in the area during this study (n = 74, Table 1) having an average pH at 7.24 ± 0.05, were transported mostly between 1000 m and 3000 m with over 60% of these recorded in spring. However, 45 dust events were acidified (acid dust) with average pH at 2.93 ± 0.87 with over 71% of those also recorded in spring. In 90% of these acidified dust events, the dust was transported either from the free troposphere or over Europe and return back to the East Mediterranean (Figs. S4 & S5). In 85% of those events the wind speed was less than 10 km h^{-1} (Fig. S6), indicating that the low wind speed could be enabled long processing times that increase the acid solubilization of dust. Significant correlation of phosphate with nss-calcium (r = 0.30, $p < 0.05$, Table S2) supports the coexistence with acid dust, while the significant correlation with nitrate (r = 0.38, $p < 0.01$, Table S2) imply that maybe nitric acid is important for the dust acidification.

The annual average concentration of nss-calcium during the acid dust events in spring was 0.76 ± 0.45 μg m^{-3} (Table 1, pH = 3.27 ± 1.27), which is lower comparing with the annual average of dust event observed during the same season (Table 1, nss-calcium 4.13 ± 3.89 μg m^{-3}, and pH = 7.27 ± 0.06). Despite the difference in nss-calcium concentrations, the phosphate concentrations between acid dust events (0.55 ± 0.37 nmol P m^{-3}) and intense dust events (0.88 ± 0.54 nmol P m^{-3}) were comparable. This suggests that the secondary phosphate fraction produced during dust acidification in the low intensity dust events could be equally important with intense dust events, occurring mainly in the spring season. Furthermore, the molar ratio PO_4^{3-}: nss-Ca^{2+} (Table 1) for the acidified dust is three times higher than the non-acidified dust and comparable with pollution transported from central Europe.

4.3. Relative importance of dust and biomass burning events on bioavailable P flux to the marine ecosystem

Atmospheric deposition of phosphate is an important nutrient source to the oligotrophic marine ecosystem of the East Mediterranean, especially during the dry season when the surface waters are strongly nutrient limited. In order to understand the relative importance of dust (acidified and not) and biomass burning events as a source of bioavailable P, the inputs from these sources are estimated.

The flux is calculated by: $F = -V_d C$, where F is the SRP flux in mol m^{-2} s^{-1}, C is the atmospheric concentration of SRP in mol m^{-3} and V_d is the deposition velocity in m s^{-1}, which depends on the size distribution of the aerosol (Spokes et al., 2001) containing the SRP but also can be dramatically influenced by pollution or the dust (Koçak et al., 2016). Since 80% of SRP in the area is associated with supermicron-sized particles during dust events (Markaki et al., 2003), a V_d of 0.02 m s^{-1} was used for the calculation of the SRP deposition during the strong dust event recorded on 23th March (Fig. 2c). With an average SRP of 1.68 ± 0.56 nmol m^{-3}, the deposition flux was calculated at 2.90 ± 0.97 μmol P m^{-2} for that event, considering the dust as an important bioavailable P source in the spring period when 60% of the events occur (Table 1). Acid processed dust events are generally low intense dust events, having an average concentration of nss-calcium of 0.78 ± 0.41 μg m^{-3}, and during the most intense acid dust event an average concentration of SRP of 0.64 ± 0.16 nmol m^{-3} was recorded; the deposition flux of SRP was calculated at 1.11 ± 0.28 μmol P m^{-2} per event.

During biomass burning episodes was used the V_d of 0.012 m s^{-1}, adopting the approach of Koçak et al. (2016), which represent a polluted atmosphere of East Mediterranean. The daily average concentration of SRP recorded on the event of 26th Aug. (Fig. 3) was at 0.84 ± 0.24 nmol m^{-3}, the deposition flux of SRP was calculated at 0.87 ± 0.25 μmol P m^{-2} per event, establishing that biomass events are an important source of bioavailable phosphorus in the area, especially in the summer period when the East Mediterranean surface waters are nutrient starved.

Dust storms in the Mediterranean and the Atlantic are anticipated to be more frequent and intense and further exacerbated from the effects of anthropogenic climate change. Also, the observed trend towards warmer and drier conditions in southern Europe is projected to continue in the next decades, possibly leading to increased risk of large fires (Turco et al., 2018). Increases in the number of fires (Tang et al., 2021) and the dust storms, would potentially enhance the atmosphere as a nutrient source of bioavailable P for the Mediterranean marine ecosystem.

5. Conclusions

During this study, a real-time automated PILS-LWCC system with a time resolution of six minutes per sample was used to measure the SRP in

atmospheric particles over the eastern Mediterranean. With that high-resolution sampling, the evolution of SRP concentration in dust aerosols during the event was recorded but also its temporal variation during biomass burning episodes. The results revealed that the Saharan dust is an important primary source of bioavailable phosphorus, while the acid dust enhances further the contribution of dust aerosol to the SRP. During the warm period, when Northerly winds prevailed, biomass burning episodes contributed significantly to soluble phosphorus delivered from atmospheric sources to the eastern Mediterranean. These inputs are comparable with acid processed dust events and are especially important for the area during the summer period, when biological productivity is strongly limited by nutrient availability.

CRediT authorship contribution statement

K.V.: conceptualization, Methodology, Writing- Original draft preparation. K.V., I.T., M.T., A.N. and K.F.: collected and analyzed data. K.V., G.K., and P.Z.: resources. K.V., N.M. and A.N., have funding acquisition. A.N., N.M., K.F., C.P. E.I. and R.W. Reviewing and Editing.

Declaration of competing interest

The authors declare that they have no known competing financial interests or personal relationships that could have appeared to influence the work reported in this paper.

Acknowledgements

KV acknowledges the financial support from the European Union's Horizon 2020 research and innovation programme under the Marie Skłodowska-Curie grant agreement No 707624. KV and NM acknowledge financial support from the ACTRIS, Research Infrastructure Action under the 7th Framework Programme (Grant Agreement No 262254). AN acknowledge support from project PyroTRACH (ERC-2016-COG) funded from H2020-EU.1.1. - Excellent Science - European Research Council (ERC), project ID 726165. KV and AN acknowledge the Swiss National Science Foundation project 192292, Atmospheric Acidity Interactions with Dust and its Impacts (AAIDI). MT, GK, PZ and NM acknowledge support by the project "PANhellenic infrastructure for Atmospheric Composition and climatE change" (MIS5021516), which is implemented under the Action "Reinforcement of the Research and Innovation Infrastructure", funded by the Operational Programme "Competitiveness, Entrepreneurship and Innovation" (NSRF 2014-2020) and co-financed by Greece and the European Union (European Regional Development Fund).

Appendix A. Supplementary data

Supplementary data to this article can be found online at https://doi.org/10.1016/j.scitotenv.2022.154263.

References

Baker, R.A., Kanakidou, M., Nenes, A., Myriokefalitakis, S., Croot, P.L., Duce, R.A., Gao, Y., Guieu, C., Ito, Akinori, Jickells, T.D., Mahowald, N.M., Middag, R., Perron, M.G., Sarin, M.M., Shelley, R., Turner, D.R., 2021. Changing atmospheric acidity as a modulator of nutrient deposition and ocean biogeochemistry. Sci. Adv. 7. https://doi.org/10.1126/sciadv.abd8800.

Barkley, E., Prospero, J.M., Mahowald, N., Hamilton, D.S., Popendorf, K.J., Oehlert, A.M., Pourmand, A., Gatineau, A., Panechou-Pulcherie, K., Blackwelder, P., Gaston, C.J., 2019. African biomass burning is a substantial source of phosphorus deposition to the Amazon, Tropical Atlantic Ocean, and Southern Ocean. Proc. Natl. Acad. Sci. 116, 16216–16221.

Capaldo, K.P., Pilinis, C., Pandis, S.N., 2000. A computationally efficient hybrid approach for dynamic gas/aerosol transfer in air quality models. Atmos. Environ. 34, 3617–3627.

Fountoukis, C., Nenes, A., 2007. ISORROPIA II: a computationally efficient thermodynamic equilibrium model for K+ - Ca2+ - Mg2+ - NH4+ - Na+ - SO42- - NO3− - Cl− - H2O aerosols. Atmos. Chem. Phys. 7, 4639–4659. https://doi.org/10.5194/acp-7-4639-2007.

Gerasopoulos, E., Kouvarakis, G., Babasakalis, P., Vrekoussis, M., Putaud, J.-P., Mihalopoulos, N., 2006. Origin and variability of particulate matter (PM10) mass concentrations over the Eastern Mediterranean. Atmos. Environ. 40, 4679–4690.

Guerzoni, S., Chester, R., Dulac, F., Herut, B., Lo¨ye-Pilot, M.D., Measures, C., Migon, C., Molinaroli, E., Moulin, C., Rossini, P., Saydam, C., Soudine, A., Ziveri, P., 1999. The role of atmospheric deposition in the biogeochemistry of the Mediterranean sea. Prog. Oceanogr. 44, 147–190.

Herut, B., Collier, R., Krom, M.D., 2002. The role of dust in supplying nitrogen and phosphorus to the Southeast Mediterranean. Limnol. Oceanorg. 47, 870–878.

Kakavas, S., Patoulias, D., Zakoura, M., Nenes, A., Pandis, S.N., 2021. Size-resolved aerosol pH over Europe during summer. Atmos. Chem. Phys. 21, 799–811. https://doi.org/10.5194/acp-21-799-2021.

Kalivitis, N., Gerasopoulos, E., Vrekoussis, M., Kouvarakis, G., Kubilay, N., Hatzianastassiou, N., Vardavas, I., Mihalopoulos, N., 2007. Dust transport over the eastern Mediterranean derived from Total Ozone Mapping Spectrometer, Aerosol Robotic Network, and surface measurements. J. Geophys. Res. 112, D03202. https://doi.org/10.1029/2006JD007510 2007.

Karl, David M., Björkman, Karin M., 2015. Dynamics of dissolved organic phosphorus. In: Hansell, Dennis A., Carlson, Craig A. (Eds.), Biogeochemistry of Marine Dissolved Organic Matter. Academic Press, Burlington, pp. 233–334.

Koçak, M., Kubilay, N., Tugrul, S., Mihalopoulos, N., 2010. Atmospheric nutrient inputs to the northern levantine basin from a long-term observation: sources and comparison with riverine inputs. Biogeosciences 7, 4037–4050. https://doi.org/10.5194/bg-7-4037-2010.

Koçak, M., Mihalopoulos, N., Tutsak, E., Violaki, K., Theodosi, C., Zarmpas, P., Kalegeri, P., 2016. Atmospheric Deposition of Macronutrients (Dissolved Inorganic Nitrogen and Phosphorous) Onto the Black Sea and Implications on Marine Productivity, pp. 1727–1739 https://doi.org/10.1175/JAS-D-15-0039.1.

Kostenidou, E., Pathak, R.K., Pandis, S.N., 2007. An algorithm for the calculation of secondary organic aerosol density combining AMS and SMPS Data. Aerosol Sci.Technol. 41, 1002–1010. https://doi.org/10.1080/02786820701666270.

Koulouri, E., Saarikoski, S., Theodosi, C., Markaki, Z., Gerasopoulos, E., Kouvarakis, G., Makela, T., Hillamo, R., Mihalopoulos, N., 2008. Chemical composition and sources of fine and coarse aerosol particles in the Eastern Mediterranean. Atmos. Environ. 42, 6542–6550.

Krom, M.D., Shi, Z., Stockdale, A., Berman-Frank, I., Giannakourou, A., Herut, B., et al., 2016. Response of the Eastern Mediterranean microbial ecosystem to dust and dust affected by acid processing in the atmosphere. Front. Mar. Sci. 3, 133. https://doi.org/10.3389/fmars.2016.00133.

Longo, A.F., Ingall, E.D., Diaz, J.M., Oakes, M., King, L.E., Nenes, A., Mihalopoulos, N., Violaki, K., Avila, A., Benitez-Nelson, C.R., 2014. P-NEXFS analysis of aerosol phosphorus delivered to the Mediterranean Sea. Geophys. Res. Lett. 41, 4043–4049.

Mahowald, N., Jickells, T.D., Baker, A.R., Artaxo, P., Benitez-Nelson, C.R., Bergametti, G., Bond, T.C., Chen, Y., Cohen, D.D., Herut, B., Kubilay, N., Losno, R., Luo, C., Maenhaut, W., McGee, K.A., Okin, G.S., Siefert, R.L., Tsukuda, S., 2008. Global distribution of atmospheric phosphorus sources, concentrations and deposition rates, and anthropogenic impacts. Glob. Biogeochem. Cycles 22, GB4026.

Markaki, Z., Oikonomou, K., Kocak, M., Kouvarakis, G., Chaniotaki, A., Kubilay, N., Mihalopoulos, N., 2003. Atmospheric deposition of inorganic phosphorus in the Levantine basin, eastern Mediterranean: spatial and temporal variability and its role in seawater productivity. Limnol. Oceanogr. 48, 1557–1568.

Mihalopoulos, N., Stephanou, E., Pilitsidis, S., Kanakidou, M., Bousquet, P., 1997. Atmospheric aerosol composition above the Eastern Mediterranean region. Tellus 49B, 314–326.

Nenes, A., Pilinis, C., Pandis, S.N., 1998. ISORROPIA: a new thermodynamic model for multiphase multicomponent inorganic aerosols. Aquat. Geochem. 4, 123–152.

Nenes, A., Krom, M.D., Mihalopoulos, N., Van Cappellen, P., Shi, Z., Bougiatioti, A., Zarmpas, P., Herut, B., 2011. Atmospheric acidification of mineral aerosols: a source of bioavailable phosphorus for the oceans. Atmos. Chem. Phys. 11, 6265–6272.

Okin, G.S., Baker, A.R., Tegen, I., Mahowald, N.M., Dentener, F.J., Duce, R.A., Galloway, J.N., Hunter, K., Kanakidou, M., Kubilay, N., Prospero, J.M., Sarin, M., Surapipith, V., Uematsu, M., Zhu, T., 2011. Impacts of atmospheric nutrient deposition on marine productivity: roles of nitrogen, phosphorus, and iron. Glob. Biogeochem. Cycles 25, GB2022. https://doi.org/10.1029/2010GB003858.

Pitta, P., Kanakidou, M., Mihalopoulos, N., Christodoulaki, S., Dimitriou, P.D., Frangoulis, C., Giannakourou, A., Kagiorgi, M., Lagaria, A., Nikolaou, P., Papageorgiou, N., Psarra, S., Santi, I., Tsapakis, M., Tsiola, A., Violaki, K., Petihakis, G., 2017. Saharan dust deposition effects on the microbial food web in the Eastern Mediterranean: a study based on a mesocosm experiment. Front. Mar. Sci. 4, 117.

Pye, H.O.T., Nenes, A., Alexander, B., Ault, A.P., Barth, M.C., Clegg, S.L., Collett Jr., J.L., Fahey, K.M., Hennigan, C.J., Herrmann, H., Kanakidou, M., Kelly, J.T., Ku, I.-T., McNeill, V.F., Riemer, N., Schaefer, T., Shi, G., Tilgner, A., Walker, J.T., Wang, T., Weber, R., Xing, J., Zaveri, R.A., Zuend, A., 2020. The acidity of atmospheric particles and clouds. Atmos. Chem. Phys. 20, 4809–4888. https://doi.org/10.5194/acp-20-4809-2020.

Sciare, J., Oikonomou, K., Favez, O., Liakakou, E., Markaki, Z., Cachier, H., Mihalopoulos, N., 2008. Long-term measurements of carbonaceous aerosols in the Eastern Mediterranean: evidence of long-range transport of biomass burning. Atmos. Chem. Phys. 8, 5551–5563. https://doi.org/10.5194/acp-8-5551-2008.

Spokes, L., Jickells, T., Jarvis, K., 2001. Atmospheric inputs of trace metals to the northeast Atlantic Ocean: the importance of southeasterly flow. Mar. Chem. 76 (4), 319–330. https://doi.org/10.1016/S0304-4203(01)00071-8.

Stein, A.F., Draxler, R.R., Rolph, G.D., Stunder, B.J.B., Cohen, M.D., Ngan, F., 2015. NOAA'S hysplit atmospheric transport and dispersion modeling system. Bull. Am. Meteorol. Soc. https://doi.org/10.1175/BAMS-D-14-00110.1.

Stockdale, A., Krom, M.D., Mortimer, R.J.G., Benning, L.G., Carslaw, K.S., Herbert, R.J., Shi, Z.B., Myriokefalitakis, S., Kanakidou, M., Nenes, A., 2016. Understanding the nature of

atmospheric acid processing of mineral dusts in supplying bioavailable phosphorus to the oceans. Proc. Natl. Acad. Sci. U. S. A. 113, 14639–14644.

Tang,, W., Llort, J., Weis,, J., Perron, M.M.G., Basart, S., Li, Z., Sathyendranath, S., Jackson, T., Rodriguez, E.S., Proemse, B.C., Bowie, A.R., Schallenberg, C., Strutton, P.G., Matear, R., Cassar, N., 2021. Widespread phytoplankton blooms triggered by 2019–2020 Australian wildfires. Nature 597, 370–375. https://doi.org/10.1038/s41586-021-03805-8.

Turco, M., Rosa-Cánovas, J.J., Bedia, J., Jerez, S., Montávez, J.P., Llasat, M.C., Provenzale, A., 2018. Exacerbated fires in Mediterranean Europe due to anthropogenic warming projected with non-stationary climate-fire models. Nat. Commun. 9, 3821. https://doi.org/10.1038/s41467-018-06358-z.

Violaki, K., Fang, T., Mihalopoulos, N., Weber, R., Nenes, A., 2016. Real-time, online automated system for measurement of water-soluble reactive phosphate ions in atmospheric particles. Anal. Chem. 88 (14), 7163–7170.

Violaki, K., Bourrin, F., Aubert, D., Kouvarakis, G., Delsaut, N., Mihalopoulos, N., 2018. Organic phosphorus in atmospheric deposition over the Mediterranean Sea: an important missing piece of the phosphorus cycle. Prog. Oceanogr. 163, 50–58.

Violaki, K., Nenes, A., Tsagkaraki, Marco Paglione, Jacquet, Stéphanie, Sempéré, Richard, Panagiotopoulos, Christos, 2021. Bioaerosols and dust are the dominant sources of organic P in atmospheric particles. npj Clim. Atmos. Sci. 4, 63. https://doi.org/10.1038/s41612-021-00215-5.

Wang, R., Balkanski, Y., Boucher, O., Ciais, P., Peñuelas, J., Tao, S., 2015. Significant contribution of combustion-related emissions to the atmospheric phosphorus budget. Nat. Geosci. 8, 48–54.